THE INFLUENCE OF STEEL MICROSTRUCTURE ON DYNAMIC FRACTURE TOUGHNESS

J. Buchar, Z. Knésl, Z. Bilek[x]

The influence of initial microstructure of low alloy weldable (C-Mo-Cr) steel on dynamic fracture toughness K_{Id} at very high loading rates is demonstrated. The results obtained within wide temperature range are compared with the K_{Id} values from Charpy instrumented tests for seven different microstructures. Dynamic elastic finite element analysis shows the limited applicability of static approach to the K_{Id} evalution and demonstrates the significance of stress wave phenomena. The problems associated with application of critical stress fracture criterion in dynamic situation are briefly outlined.

INTRODUCTION

The application of a dynamic fracture mechanics approach to the safety assessment of dynamically loaded engineering structures requires the availability of relevant data. Namely it is necessary to have information on dynamic fracture toughness K_{Id} associated with rapid loading conditions that can occur during operation since K_{Id} is a decreasing function of loading rate $\dot{K}_I$ for the most of structural steels. In this paper we apply the method developed by Klepaczko (1,2) to study the temperature dependence of K_{Id} for various complex microstructures in C-Cr-Mo steel. The experimental data were evaluated using the static and dynamic finite element procedure developed by Kuna et al (3) and by Bilek et al (4).

In order to understand our experimental findings we have had to establish a detailed theoretical description of the stress field ahead of the crack by means of dynamic elastic-plastic computations for the linear hardening material. We have attempted to predict the K_{Id} values with the aid of a critical stress criterion which has already a sound theoretical basis created by Knott et al (5,6) for static fracture toughness K_{IC}.

Institute of Physical Metallurgy, Czechoslovak Academy of Sciences, Brno

EXPERIMENTAL PROCEDURE

Our steel having chemical composition 0.13% C, 0.61% Mn, 0.10% P, 0.28% Si, 0.007% S, 2.39% Cr, 0.22% Ni, 0.95% Mo, 0.05% Cu was thermaly treated to seven different microstructure stages described in Table 1.

TABLE 1 - Description of initial microstructural conditions

Microstructure	Heat treatment	Nil ductility temperature NDT, °C	Static yield stress MPa
MI	As received	-15	444
MII	Q, 940°C/water	-25	1001
MIII	Q,T 940°C/water/550°C	-15	1034
MIV	Q,T 940°C/water/640°C	-35	729
MV	Q,T 940°C/water/720°C	-50	572
MVI	Normalizing 940°C/air T 720°C	-15	524
MVII	Normalizing 940°C/air T 780°C	-30	385

Experimental set up follows from Figure 1. WLCT specimen with geometry shown in Figure 2 is placed between two steel bars. The first loading bar produces a stress puls σ_I (t) with duration time of λ_I = 52μs , σ_T (t) is a stress pulse transmited to the second bar. To evaluate the K_{Id} values we used procedure given in references (1,2) completed by our finite element computations.

FINITE ELEMENT ANALYSIS

All calculations have been done by finite element method for the geometry given in Figure 2 and ratio a/w = 0.5. The problem was treated as plane one. The values of static stress intensity factor K_I^S were determined by means of hybrid technique in reference (3).

For dynamic calculations, the program BKDYN from reference (4) was used to solve elastic and elastic-plastic problems on ICL 2950 computer. This program makes use of a four node quadrilateral elements and for time integration the explicit central difference method is implemented with automatic selection and adjustment of time step. The loading was modelled by real opening force F(t) shown in Figure 3 and the values of dynamic stress intensity factor $K_I(t)$ was found from the displacements u_y . The boundary conditions correspond to free surface specimen during the impact loading. Typical results are summarized in Figure 3 for data corresponding to microstructure MII at T = 20°C, mesh having 2500 elements and 2660 nodal points for one half of the specimen.

RESULTS AND DISCUSSION

The results shown in Figure 3 indicate a great difference between K_I^s and $K_I(t)$ so one should be very carefull evaluating K_{Id} values according the procedures based on static analysis as recommended in references (1,2). The extensive plastic zone development studies in the particular form of Figure 4 suggest that despite unusually small specimens the plane strain conditions prevail and our K_{Id} data are valid from this point of view. Figures 3,4 and 5 demonstrate the complicated way of crack tip loading during the test. Figures 7 to 9 show temperature dependence of K_{Id} for all microstructures investigated. Considering the scatter of experimental data the inexpressive decrease of K_{Id} in comparison with Charpy test data can not be interpreted clearly in terms of $\dot{K}_I$ increase from 10^5 to 10^6 MPa $m^{1/2}s^{-1}$ - e.g. see Figure 9b. Therefore for microstructures MI, MIV and MVII as well, the Charpy K_{Id} values determined in accordance with ASTM recomendations represent the minimum on $K_{Id}(\dot{K})$ curves. This conclusion is also valid for microstructures MV (tempered martensite) and MVI (bainit) below NDT. But for T > NDT Hopkinson split bar technique data lie substantialy below Charpy K_{Id} values. For martensite microstructures (MII,MIII) the K_{Id} values at $\dot{K}_I = 10^6$ MPa $m^{1/2}s^{-1}$ are above the K_{Id} data at $\dot{K}_I = 10^5$MPa $m^{1/2}s^{-1}$ for $T > -50^oC$. In general, it appears that Charpy impact data represent good approximations for the minimum of dynamic crack initiation toughness important in engineering desing.

Knott et al (5,6) have presented an analysis which related σ_{CF} to K_{IC}. Essentially this approach was adopted in this paper for K_{Id} interpretation. The cleavage stress σ_{CF} and process zone size R_o over which this stress is reached were found following paper by Holzmann et al (7). For example, for microstructure MII, σ_{CF} = 1600 MPa and R_o = 0.065mm. Assuming that both quantities σ_{CF} and R_o are independent of strain rate and temperature we find with the help of Figure 6 that fracture criterion $\sigma_{yy} = \sigma_{CF}$ is met for $x = R_o$ at time $t = 15\mu s$. On the other hand at this time the dynamic stress intensity (Figure 3) reaches the value of $K_I(t)$ = = 40 MPa $m^{1/2}$ which is below K_{Id} = 203 MPa $m^{1/2}$. This value of K_{Id} is reached later at $t = 25.5\,\mu s$, which supports the existence of incubation time (10.5μs) proposed by Kalthoff and Shockey (8) to initiate a fracture by stress pulse loading. It appears that K_{Id} is not controlled only by σ_{CF} and R_o but also by incubation time necessary to start a crack. Stress analysis to this check hypothesis at other temperature (different loading) is in progress.

SYMBOLS USED

a = crack length (mm)

A = bar crossection (m^2)

E = Young modulus (MPa)

F(t) = applied force (kN)

2H = height of the specimen (mm)

K_I^s, $K_I(t)$ = static and dynamic stress intensity factor ($MPam^{1/2}$)

$\dot{K}_I$ = loading rate ($MPam^{1/2}s^{-1}$)

K_{IC}, K_{Id} = static and dynamic fracture toughness ($MPam^{1/2}$)
NDT = nil ductility transition temperature (^{o}C)
R_o = process zone size (mm)
t = time (us)
T = temperature (^{o}C)
uy = displacement component in y direction (mm)
w = length of specimen (mm)
x = distance from a crack tip
α = wedge angle
λ_I = loading puls duration
$\sigma_I(t)$, $\sigma_I(t)$, $\sigma_R(t)$ = loading, transmitted and reflected stress pulse (MPa)
σ_{yy} = normal stress component in y direction (MPa)
σ_{CF} = critical cleavage stress (MPa)

REFERENCES

1. Klepaczko,J.R., 1982, J.Eng.Mat.Tech., 104, 29
2. Klepaczko,J.R., 1979,"Application of the Split Hopkinson Pressure bar to fracture dynamics", Physics Conference Ser. No 47, London England.
3. Kuna,M. et al. 1981, Maschinenbautechnik, 30, 75
4. Bilek,Z. et al. 1982, Metallic Materials, 20, in press.
5. Knott,J.F. et al. 1973, J. Mech.Phys Solids, 21, 395
6. Knott,J.F., 1977, "Micro-mechanismus of fracture" ICF4 Congress Proceedings, Waterloo, Canada.
7. Holzmann,M. et al., 1981 Int J.Pressure Ves.Pip., 9, 1
8. Kalthoff,J.F. and Shockey, D.A., 1977, J.Appl.Phys.,48, 986

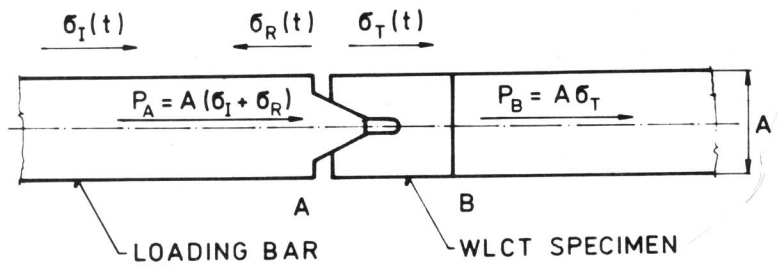

Figure 1 Schematic experimental set up for K_{Id} measurements

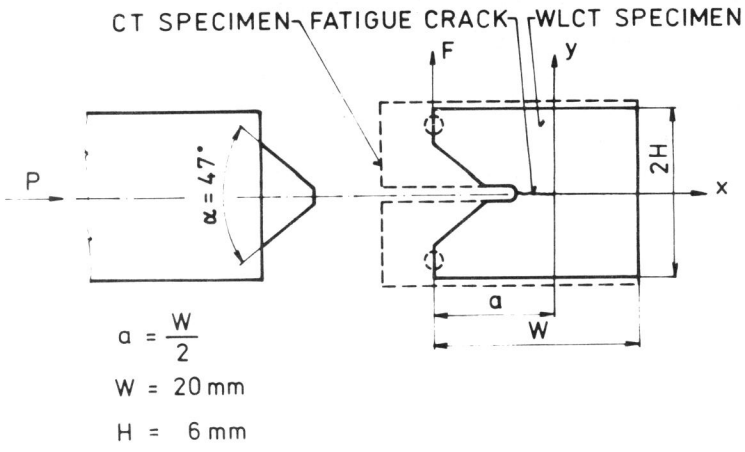

Figure 2 Wedge loaded compact tension WLCT specimen geometry

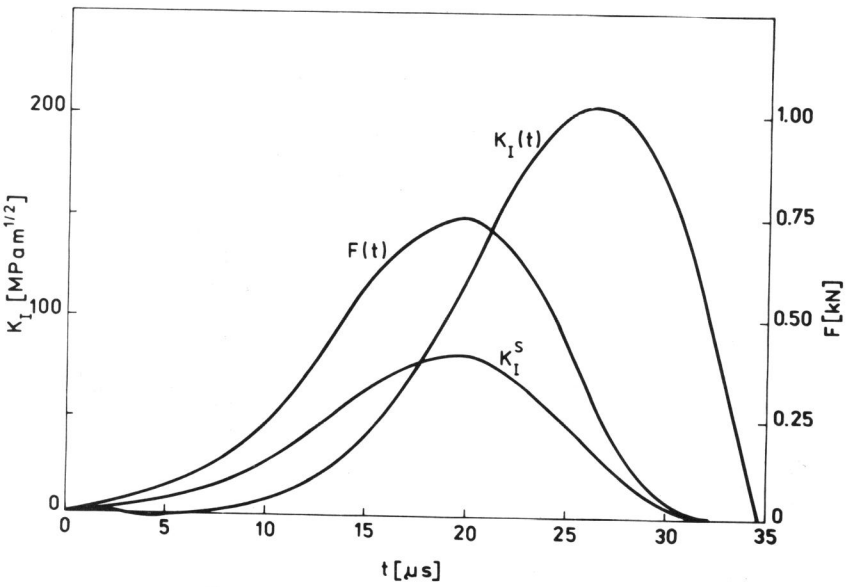

Figure 3 Static K_I^S, dynamic $K_I(t)$ stress intensity factor and loading pulse per 1 mm thickness F(t) vs. time

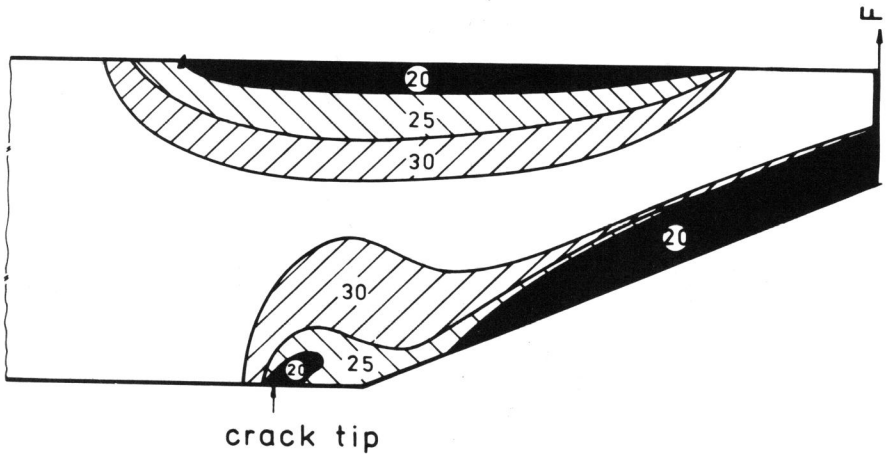

Figure 4 Plastic zone development for 20, 25 and 30 μs for linear hardening with secant modulus E/165

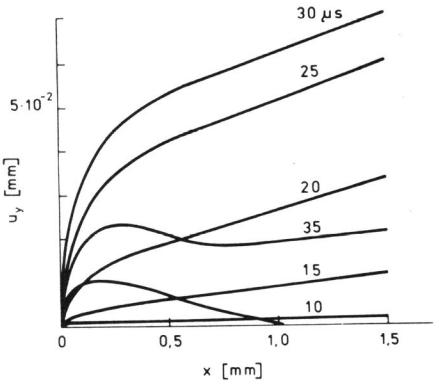

Figure 5 Crack profiles

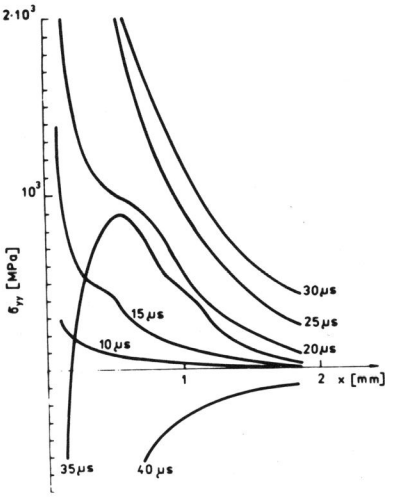

Figure 6 Normal stress σ_{yy} behaviour at the crack tip

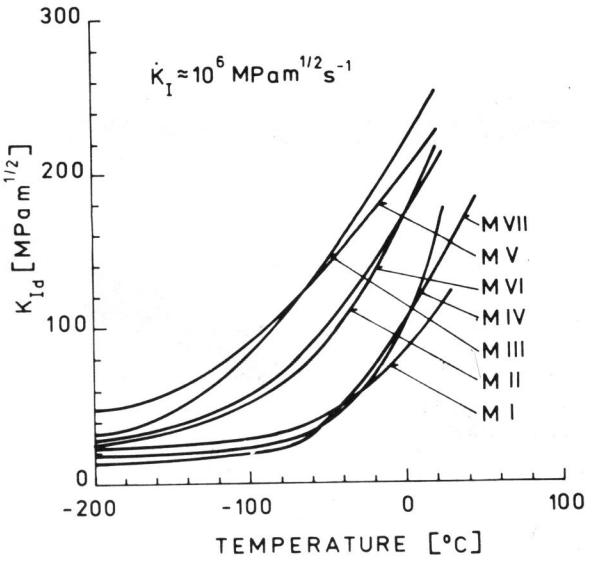

Figure 7 Temperature dependence of K_{Id} for various microstructures

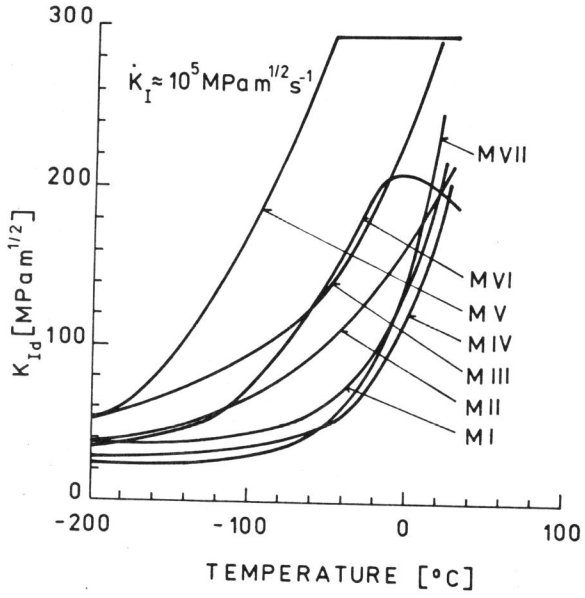

Figure 8 Instrumented Charpy K_{Id} data

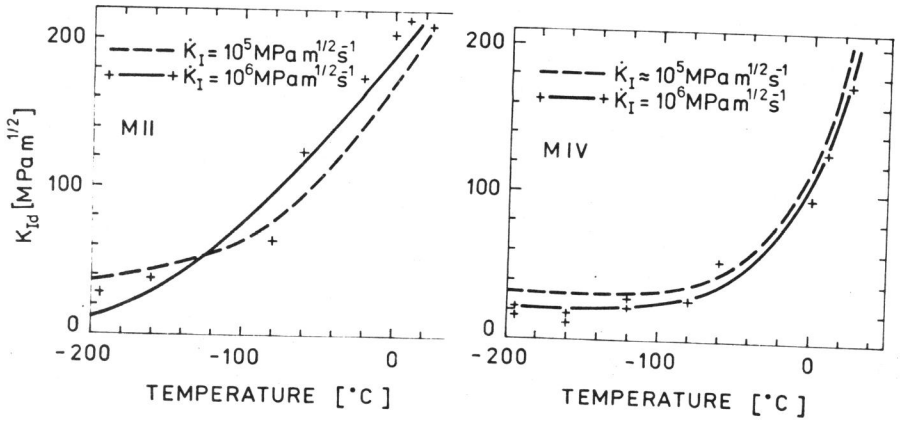

Figure 9 Comparison of experimental K_{Id} data for two microstructures at two loading rates